Measuring the Small-Scale Power Spectrum of Cosmic Density Fluctuations through 21 cm Tomography Prior to the Epoch of Structure Formation

Abraham Loeb[1] and Matias Zaldarriaga[2]

[1]*Astronomy Department, Harvard University, 60 Garden Street, Cambridge, Massachusetts 02138, USA*
[2]*Physics Department, Harvard University, 17 Oxford Street, Cambridge, Massachusetts 0213, USA*

(Received 4 December 2003; published 25 May 2004)

The thermal evolution of the cosmic gas decoupled from that of the cosmic microwave background (CMB) at a redshift $z \sim 200$. Afterwards and before the first stars had formed, the cosmic neutral hydrogen absorbed the CMB flux at its resonant 21 cm spin-flip transition. We calculate the evolution of the spin temperature for this transition and the resulting anisotropies that are imprinted on the CMB sky due to linear density fluctuations during this epoch. These anisotropies, at an observed wavelength of $10.56[(1+z)/50]$ m, contain an amount of information that is orders of magnitude larger than any other cosmological probe.

DOI: 10.1103/PhysRevLett.92.211301 PACS numbers: 98.70.Vc, 95.30.Jx, 98.65.–r, 98.80.Es

Introduction.—The small residual fraction of free electrons after cosmological recombination coupled the temperature of the cosmic gas to that of the cosmic microwave background (CMB) down to a redshift, $z \sim 200$ [1]. Subsequently, the gas temperature dropped adiabatically as $T_{\rm gas} \propto (1+z)^2$ below the CMB temperature $T_\gamma \propto (1+z)$. The gas heated up again after being exposed to the photoionizing ultraviolet light emitted by the first stars during the *reionization epoch* at $z \lesssim 20$ (see review in [2]). Prior to the formation of the first stars, the cosmic neutral hydrogen must have resonantly absorbed the CMB flux through its spin-flip 21 cm transition [3–6]. The linear density fluctuations at that time should have imprinted anisotropies on the CMB sky at an observed wavelength of $21.12[(1+z)/100]$ m. In this Letter, we calculate the power spectrum of these anisotropies and assess the significance of their potential detection. A direct measurement of the amplitude of inhomogeneities on small spatial scales would constrain any possible tilt or running of the spectral index of the power spectrum as recently suggested by Wilkinson Microwave Anisotropy Probe (WMAP) [7], or any suppression of power on small scales due to a warm dark matter component in the cosmic mass budget [8].

Spin temperature history.—We start by calculating the history of the spin temperature, T_s, defined through the ratio between the number densities of hydrogen atoms in the excited and ground state levels, $n_1/n_0 = (g_1/g_0)\exp\{-T_\star/T_s\}$, where subscripts 1 and 0 correspond to the excited and ground state levels of the 21 cm transition, $(g_1/g_0) = 3$ is the ratio of the spin degeneracy factors of the levels, $n_{\rm H} = (n_0 + n_1) \propto (1+z)^3$ is the total hydrogen density, and $T_\star = 0.068$ K is the temperature corresponding to the energy difference between the levels. The time evolution of the density of atoms in the ground state is given by

$$\left(\partial_t + 3\frac{\dot a}{a}\right) n_0 = -n_0(C_{01} + B_{01}I_\nu) + n_1(C_{10} + A_{10} + B_{10}I_\nu), \quad (1)$$

where $a(t) = (1+z)^{-1}$ is the cosmic scale factor, A's and B's are the Einstein rate coefficients, C's are the collisional rate coefficients, and I_ν is the blackbody intensity in the Rayleigh-Jeans tail of the CMB, namely, $I_\nu = 2k_B T_\gamma/\lambda^2$ with $\lambda = 21$ cm [9]. The $0 \rightarrow 1$ transition rates can be related to the $1 \rightarrow 0$ transition rates by the requirement that in thermal equilibrium with $T_s = T_\gamma = T_{\rm gas}$, the right-hand side of Eq. (1) should vanish with the collisional terms balancing each other separately from the radiative terms. The Einstein coefficients are $A_{10} = 2.85 \times 10^{-15}\ {\rm s}^{-1}$, $B_{10} = (\lambda^3/2hc)A_{10}$, and $B_{01} = (g_1/g_0)B_{10}$ [3,9]. The collisional deexcitation rates can be written as $C_{10} = \frac{4}{3}\kappa(1-0)n_{\rm H}$, where $\kappa(1-0)$ is tabulated as a function of $T_{\rm gas}$ [10].

Equation (1) can be simplified to the form

$$\frac{d\Upsilon}{dz} = -[H(1+z)]^{-1} \times [-\Upsilon(C_{01} + B_{01}I_\nu) + (1-\Upsilon)(C_{10} + A_{10} + B_{10}I_\nu)], \quad (2)$$

where $\Upsilon \equiv n_0/n_{\rm H}$, $H \approx H_0\sqrt{\Omega_m}(1+z)^{3/2}$ is the Hubble parameter at high redshifts (with a present-day value of H_0), and Ω_m is the density parameter of matter. The upper panel of Fig. 1 shows the results of integrating Eq. (2). Both the spin temperature and the kinetic temperature of the gas track the CMB temperature down to $z \sim 200$. Collisions are efficient at coupling T_s and $T_{\rm gas}$ down to $z \sim 70$, and so the spin temperature follows the kinetic temperature around that redshift. At much lower redshifts, the Hubble expansion makes the collision rate subdominant relative to the radiative coupling rate to

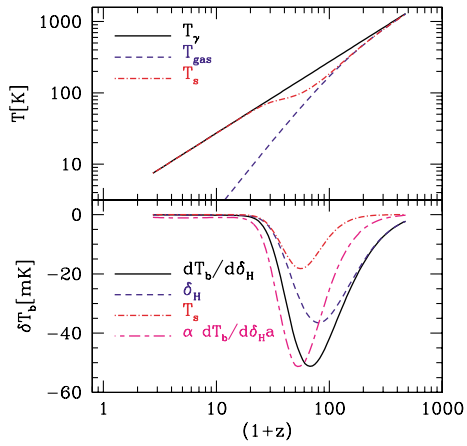

FIG. 1 (color online). Upper panel: Evolution of the gas, CMB, and spin temperatures with redshift [4]. Lower panel: $dT_b/d\delta_H$ as a function of redshift. The separate contributions from fluctuations in the density and the spin temperature are depicted. We also show $dT_b/d\delta_H a \propto dT_b/d\delta_H \times \delta_H$, with an arbitrary normalization. Throughout this Letter, we assume the standard set of cosmological parameters for a universe dominated by cold dark matter and a cosmological constant (ΛCDM) [6].

the CMB, and so T_s tracks T_γ again. Consequently, there is a redshift window between $30 \lesssim z \lesssim 200$, during which the cosmic hydrogen absorbs the CMB flux at its resonant 21 cm transition. Coincidentally, this redshift interval precedes the appearance of collapsed objects [2] and so its signatures are not contaminated by nonlinear density structures or by radiative or hydrodynamic feedback effects from stars and quasars.

During the period when the spin temperature is smaller than the CMB temperature, neutral hydrogen atoms absorb CMB photons. The resonant 21 cm absorption reduces the brightness temperature of the CMB by

$$T_b = \tau(T_s - T_\gamma)/(1+z), \tag{3}$$

where the optical depth for resonant 21 cm absorption is

$$\tau = \frac{3c\lambda^2 h A_{10} n_{\rm H}}{32\pi k_B T_s H(z)}. \tag{4}$$

Small inhomogeneities in the hydrogen density $\delta_H \equiv (n_{\rm H} - \bar{n}_{\rm H})/\bar{n}_{\rm H}$ result in fluctuations of the 21 cm absorption through two separate effects. An excess of neutral hydrogen directly increases the optical depth and also alters the evolution of the spin temperature. We can write an equation for the resulting evolution of Υ fluctuations,

$$\frac{d\delta\Upsilon}{dz} = [H(1+z)]^{-1}\{[C_{10} + C_{01} + (B_{01} + B_{10})I_\nu]\delta\Upsilon + [C_{01}\Upsilon - C_{10}(1-\Upsilon)]\delta_H\}, \tag{5}$$

leading to spin temperature fluctuations,

$$\frac{\delta T_s}{\bar{T}_s} = -\frac{1}{\ln[3\Upsilon/(1-\Upsilon)]}\frac{\delta\Upsilon}{\Upsilon(1-\Upsilon)}. \tag{6}$$

The resulting brightness temperature fluctuations can be related to the derivative,

$$\frac{dT_b}{d\delta_H} \equiv \bar{T}_b + \frac{T_\gamma \bar{T}_b}{(\bar{T}_s - T_\gamma)}\frac{\delta T_s}{\bar{T}_s \delta_H}, \tag{7}$$

through $\delta T_b = (dT_b/d\delta_H)\delta_H$. We include all fluctuations caused by δ_H except for the variation in C_{ij} due to fluctuations in $T_{\rm gas}$, which is very small [10]. Figure 1 shows $dT_b/d\delta_H$ as a function of redshift, including the two contributions to $dT_b/d\delta_H$, one originating directly from density fluctuations and the second from the associated changes in the spin temperature [4]. Both contributions have the same sign, because an increase in density raises the collision rate and lowers the spin temperature, and so it allows T_s to better track $T_{\rm gas}$. Since δ_H grows with time as $\delta_H \propto a$, the signal peaks at $z \sim 50$, a slightly lower redshift than the peak of $dT_b/d\delta_H$.

Next we calculate the angular power spectrum of the brightness temperature on the sky, resulting from density perturbations with a power spectrum $P_\delta(k)$,

$$\langle \delta_H(\mathbf{k}_1)\delta_H(\mathbf{k}_2)\rangle = (2\pi)^3\delta^D(\mathbf{k}_1 + \mathbf{k}_2)P_\delta(k_1), \tag{8}$$

where $\delta_H(\mathbf{k})$ is the Fourier transform of the hydrogen density field, $\mathbf{k}$ is the comoving wave vector, and $\langle\cdots\rangle$ denotes an ensemble average (following the formalism described in [6]). The 21 cm brightness temperature observed at a frequency ν, corresponding to a distance r along the line of sight, is given by

$$\delta T_b(\mathbf{n}, \nu) = \int dr W_\nu(r)\frac{dT_b}{d\delta_H}\delta_H(\mathbf{n}, r), \tag{9}$$

where $\mathbf{n}$ denotes the direction of observation, $W_\nu(r)$ is a narrow function of r that peaks at the distance corresponding to ν. The details of this function depend on the characteristics of the experiment. The brightness fluctuations in Eq. (9) can be expanded in spherical harmonics with expansion coefficients $a_{lm}(\nu)$. The angular power spectrum of map $C_l(\nu) = \langle|a_{lm}(\nu)|^2\rangle$ can be expressed in terms of the 3D power spectrum of fluctuations in the density $P_\delta(k)$,

$$C_l(\nu) = 4\pi\int\frac{d^3k}{(2\pi)^3}P_\delta(k)\alpha_l^2(k,\nu), \qquad \alpha_l(k,\nu) = \int dr W_{r_0}(r)\frac{dT_b}{d\delta_H}(r)j_l(kr). \tag{10}$$

Our calculation ignores inhomogeneities in the hydrogen ionization fraction, since they freeze at the earlier recombination epoch ($z \sim 10^3$), and so their amplitude is more than an order of magnitude smaller than δ_H at $z \lesssim 100$. The peculiar velocity and gravitational potential perturbations induce redshift distortion effects that are of order $\sim(H/ck)$ and $\sim(H/ck)^2$ smaller than δ_H for the high-l modes of interest here. These effects are expected to be washed out within realistically broadband filters.

Figure 2 shows the angular power spectrum at various redshifts. The ability to probe the small-scale power of density fluctuations is limited only by the Jeans scale, below which the dark matter inhomogeneities are washed out by the finite pressure of the gas. Interestingly, the cosmological Jeans mass reaches its minimum value, $\sim 3 \times 10^4 M_\odot$, within the redshift interval of interest here [2]. During the epoch of reionization, photoionization heating raises the Jeans mass by several orders of magnitude and broadens spectral features, thus limiting the ability of other probes of the intergalactic medium, such as the Lyα forest, from accessing the same very low mass scales. The 21 cm tomography has the additional advantage of probing the majority of the cosmic gas, instead of the trace amount ($\sim 10^{-5}$) of neutral hydrogen probed by the Lyα forest after reionization. Similar to the primary CMB anisotropies, the 21 cm signal is simply shaped by gravity, adiabatic cosmic expansion, and well-known atomic physics, and is not contaminated by complex astrophysical processes that affect the intergalactic medium at $z \lesssim 30$.

The small-scale power spectrum.—In most models of inflation, the evolution of the Hubble parameter during inflation leads to departures from a scale-invariant spectrum that are of order $1/N_{\rm efold}$ with $N_{\rm efold} \sim 60$ being the number of e-folds between the time when the scale of our horizon was of order the horizon during inflation and the end of inflation [11]. Recent WMAP data combined with other measures of the power on smaller scales suggest that the power spectrum changes with scale much faster than inflation would have predicted [7], although this result is still somewhat controversial. Independent hints that the standard ΛCDM model may have too much power on galactic scales have inspired several proposals for suppressing the power on small scales. Examples include the possibility that the dark matter is warm and it decoupled while being relativistic so that its free streaming erased small-scale power [8], or direct modifications of inflation that produce a cutoff in the power on small scales [12]. An unavoidable collisionless component of the cosmic mass budget beyond cold dark matter is provided by massive neutrinos (see [13] for a review). Particle physics experiments established the mass splittings among different species, which translate into a lower limit on the fraction of the dark matter accounted for by neutrinos of $f_\nu > 0.3\%$, while current constraints based on galaxies as tracers of the small-scale power imply $f_\nu < 12\%$ [14].

In Fig. 3 we show the 21 cm power spectrum for various models that differ in their level of small-scale power. It is clear that a precise measurement of the 21 cm power spectrum will dramatically improve current constraints on alternatives to the standard ΛCDM spectrum.

Unprecedented information.—The 21 cm signal contains a wealth of information about the initial fluctuations. A full sky map at a single photon frequency measured up to $l_{\rm max}$, can probe the power spectrum up to $k_{\rm max} \sim (l_{\rm max}/10^4)\ {\rm Mpc}^{-1}$. Such a map contains $l_{\rm max}^2$ independent samples. By shifting the photon frequency, one may obtain many independent measurements of the power. When measuring a mode l, which corresponds to a wave number $k \sim l/r$, two maps at different photon frequencies will be independent if they are separated in radial distance by $1/k$. Thus, an experiment that covers a spatial range Δr can probe a total of $k\Delta r \sim l\Delta r/r$ independent maps. An experiment that detects the 21 cm signal over a range $\Delta\nu$ centered on a frequency ν is sensitive to $\Delta r/r \sim 0.5(\Delta\nu/\nu)(1+z)^{-1/2}$, and so it measures a total of $N_{21\,{\rm cm}} \sim 3 \times 10^{16}(l_{\rm max}/10^6)^3(\Delta\nu/\nu) \times (z/100)^{-1/2}$ independent samples.

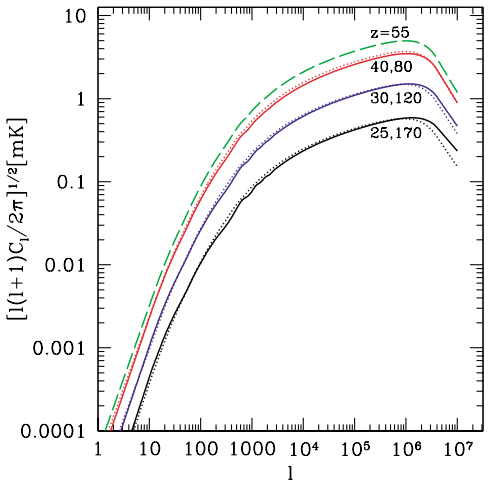

FIG. 2 (color online). Angular power spectrum of 21 cm anisotropies on the sky at various redshifts. From top to bottom, $z = 55,\ 40,\ 80,\ 30,\ 120,\ 25,\ 170$.

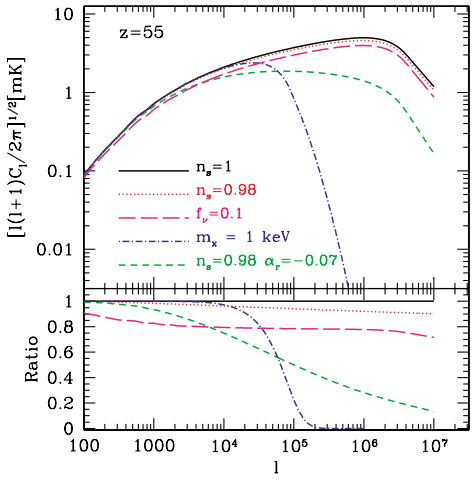

FIG. 3 (color online). Upper panel: Power spectrum of 21 cm anisotropies at $z = 55$ for a ΛCDM scale-invariant power spectrum, a model with $n = 0.98$, a model with $n = 0.98$ and $\alpha_r \equiv \frac{1}{2}(d^2 \ln P/d \ln k^2) = -0.07$, a model of warm dark matter particles with a mass of 1 keV, and a model in which $f_\nu = 10\%$ of the matter density is in three species of massive neutrinos with a mass of 0.4 eV each. Lower panel: Ratios between the different power spectra and the scale-invariant spectrum.

This detection capability cannot be reproduced even remotely by other techniques. For example, the primary CMB anisotropies are damped on small scales (through the so-called Silk damping), and probe only modes with $l \leq 3000$ ($k \leq 0.2\,\mathrm{Mpc}^{-1}$). The total number of modes available in the full sky is $N_{\mathrm{cmb}} = 2l_{\mathrm{max}}^2 \sim 2 \times 10^7 (l_{\mathrm{max}}/3000)^2$, including both temperature and polarization information.

Detectability of signal.—The sensitivity of an experiment depends strongly on its particular design, involving the number and distribution of the antennas for an interferometer. Crudely speaking, the uncertainty in the measurement of $[l(l+1)C_l/2\pi]^{1/2}$ is dominated by noise, N_ν, which is controlled by the sky brightness I_ν at the observed frequency ν [6],

$$N_\nu \sim 0.4\ \mathrm{mK}\left(\frac{I_\nu}{5 \times 10^5\ \mathrm{Jy\,sr}^{-1}}\right)\left(\frac{l_{\mathrm{min}}}{35}\right)\left(\frac{5000}{l_{\mathrm{max}}}\right)\left(\frac{0.016}{f_{\mathrm{cover}}}\right) \times \left(\frac{1\ \mathrm{yr}}{t_0}\right)^{1/2}\left(\frac{\Delta\nu}{\nu}\right)^{-1/2}\left(\frac{50\ \mathrm{MHz}}{\nu}\right)^{5/2}, \quad (11)$$

where l_{min} is the minimum observable l as determined by the field of view of the instruments, l_{max} is the maximum observable l as determined by the maximum separation of the antennae, f_{cover} is the fraction of the array area that is covered by telescopes, t_0 is the observation time, and $\Delta\nu$ is the frequency range over which the signal can be detected. The numbers adopted above are appropriate for the inner core of the LOFAR array (http://www.lofar.org), planned for initial operation in 2006. The predicted signal is $\sim$1 mK, and so a year of integration or an increase in the covering fraction are required to observe it with LOFAR. Other experiments whose goal is to detect 21 cm fluctuations include SKA (http://www.skatelescope.org) and PAST (http://astrophysics.phys.cmu.edu/~jbp). The main challenge in detecting the predicted signal involves its appearance at low frequencies where the sky noise is high. Proposed space-based instruments [15] avoid the terrestrial radio noise and the increasing atmospheric opacity at $\nu \lesssim 20$ MHz (corresponding to $z \gtrsim 70$).

Conclusions.—The 21 cm absorption is replaced by 21 cm emission from neutral hydrogen as soon as the intergalactic medium is heated above the CMB temperature during the epoch of reionization [16]. Once most of the cosmic hydrogen is reionized at z_{reion}, the 21 cm signal is diminished. The optical depth for free-free absorption after reionization, $\sim 0.1[(1+z_{\mathrm{reion}})/20]^{5/2}$, modifies only slightly the expected 21 cm anisotropies. Gravitational lensing should modify the power spectrum [17] at high l, but can be separated as in standard CMB studies (see [18] and references therein). The 21 cm signal should be simpler to clean as it includes the same lensing foreground in independent maps obtained at different frequencies.

The large number of independent modes probed by the 21 cm signal would provide a measure of non-Gaussian deviations to a level of $\sim N_{21\,\mathrm{cm}}^{-1/2}$, constituting a test of the inflationary origin of the primordial inhomogeneities which are expected to possess deviations $\gtrsim 10^{-6}$ [19].

This work was supported in part by NASA Grant No. NAG 5-13292, NSF Grants No. AST-0071019, No. AST-0204514 (for A. L.) and by NSF Grants No. AST-0098606, No. PHY-0116590, and the David and Lucille Packard Foundation (for M. Z.).

[1] P. J. E. Peebles, *Principles of Physical Cosmology* (Princeton University Press, Princeton, NJ, 1993), pp. 176–177.
[2] R. Barkana and A. Loeb, Phys. Rep. **349**, 125 (2001).
[3] G. B. Field, Astrophys. J. **129**, 536 (1959).
[4] D. Scott and M. J. Rees, Mon. Not. R. Astron. Soc. **247**, 510 (1990).
[5] P. Tozzi, P. Madau, A. Meiksin, and M. J. Rees, Astrophys. J. **528**, 597 (2000); N. Y. Gnedin and P. A. Shaver, e-print astro-ph/0312005.
[6] M. Zaldarriaga, S. Furlanetto, and L. Hernquist, e-print astro-ph/0311514.
[7] D. N. Spergel *et al.*, Astrophys. J. Suppl. Ser. **148**, 175 (2003).
[8] P. Bode, J. P. Ostriker, and N. Turok, Astrophys. J. **556**, 93 (2001); R. Barkana, Z. Haiman, and J. P. Ostriker, Astrophys. J. **558**, 482 (2001).
[9] G. B. Rybicki and A. P. Lightman, *Radiative Processes in Astrophysics* (Wiley, New York, 1979), pp. 29–32.
[10] A. C. Allison and A. Dalgarno, Astrophys. J. **158**, 423 (1969); B. Zygelman and A. Dalgarno (to be published).
[11] A. R. Liddle and D. H. Lyth, *Cosmological Inflation and Large-Scale Structure* (Cambridge University Press, Cambridge, 2000).
[12] M. Kamionkowski and A. R. Liddle, Phys. Rev. Lett. **84**, 4525 (2000).
[13] E. T. Kearns, Frascati Phys. Ser. **28**, 413 (2002); J. N. Bahcall and C. Pena-Garay, J. High Energy Phys. **0311** (2003) 004.
[14] M. Tegmark *et al.*, e-print astro-ph/0310723 [Phys. Rev. D (to be published).
[15] N. E. Kassim and K. W. Weiler, *Low Frequency Astrophysics from Space* (Springer-Verlag, New York, 1990); R. G. Stone *et al.*, *Radio Astronomy at Long Wavelengths* (American Geophysical Union, Washington, DC, 2000); see also http://rsd-www.nrl.navy.mil/7213/weiler/lfraspce.html.
[16] X. Chen and J. Miralda-Escudé, Astrophys. J. **602**, 1 (2004).
[17] U-L. Pen, New Astron **9**, 417 (2004).
[18] U. Seljak and M. Zaldarriaga, Phys. Rev. Lett. **82**, 2636 (1999); W. Hu, Astrophys. J. **556**, 93 (2001); C. M. Hirata and U. Seljak, Phys. Rev. D **67**, 043001 (2003).
[19] J. M. Maldacena, J. High Energy Phys. **0305** (2003) 013.